1 **Nintedanib ameliorates experimental pulmonary arterial hypertension via**

2 **inhibition of endothelial mesenchymal transition and smooth muscle cell proliferation**

3

4

5 Takeo Tsutsumi[1], Tetsutaro Nagaoka[1], Takashi Yoshida[1], Lei Wang[1],

6 Sachiko Kuriyama[1], Yoshifumi Suzuki[1], Yuichi Nagata[1],

7 Norihiro Harada[1], Yuzo Kodama[1], Fumiyuki Takahashi[1], Yoshiteru Morio[2],

8 and Kazuhisa Takahashi[1].

9

10 [1] Department of Respiratory Medicine, Juntendo University Faculty of Medicine & Graduate

11 School of Medicine, 3-1-3 Hongo Bunkyo-ku, Tokyo 113-8431, Japan.

12 [2] Department of Respiratory Medicine, National Hospital Organization Tokyo National

13 Hospital, 3-1-1 Takeoka Kiyose-shi, Tokyo 204-8585, Japan.

14

15 **Short title:**

16 Nintedanib for experimental pulmonary arterial hypertension

17

18 **Corresponding Author:**

19 Tetsutaro Nagaoka MD PhD

20 Department of Respiratory Medicine, Juntendo University Graduate School of Medicine

21 3-1-3 Hongo Bunkyo-ku, Tokyo 113-8431, Japan.

22 Tel: +81-3-5802-1063

23 Fax: +81-3-5802-1617

24 E-mail: jnagaoka@juntendo.ac.jp

25

30

31

32   **Abstract**

33   Neointimal lesion and medial wall thickness of pulmonary arteries (PAs) are common

34   pathological findings in pulmonary arterial hypertension (PAH). Platelet-derived growth

35   factor (PDGF) and fibroblast growth factor (FGF) signaling contribute to intimal and medial

36   vascular remodeling in PAH. Nintedanib is a tyrosine kinase inhibitor whose targets include

37   PDGF and FGF receptors. Although the beneficial effects of nintedanib were demonstrated

38   for human idiopathic pulmonary fibrosis, its efficacy for PAH is still unclear. Thus, we

39   hypothesized that nintedanib is a novel treatment for PAH to inhibit the progression of

40   vascular remodeling in PAs. The inhibitory effects of nintedanib were evaluated both in

41   endothelial mesenchymal transition (EndMT)-induced human pulmonary microvascular

42   endothelial cells (HPMVECs) and human pulmonary arterial smooth muscle cells

43   (HPASMCs) stimulated by growth factors. We also tested the effect of chronic nintedanib

44   administration on a PAH rat model induced by Sugen5416 (a VEGF receptor inhibitor)

45   combined with chronic hypoxia. Nintedanib was administered from weeks 3 to 5 after

46   Sugen5416 injection, and pulmonary hemodynamics and PAs pathology were evaluated.

47   Nintedanib attenuated the expression of mesenchymal markers in EndMT-induced

48   HPMVECs and HPASMCs proliferation. Phosphorylation of PDGF and FGF receptors was

49   augmented both in both intimal and medial lesions of PAs. Nintedanib blocked these

50   phosphorylation, improved hemodynamics and reduced vascular remodeling involving

51   neointimal lesions and medial wall thickening in PAs. Additionally, expressions Twist1,

52   transcription factors associated with EndMT, in lung tissue was significantly reduced by

53   nintedanib. These results suggest that nintedanib may be a novel treatment for PAH with

54   anti-vascular remodeling effects.

55

56   Word count: 247

57

Introduction

58

59   The pathogenesis of pulmonary arterial hypertension (PAH) involves abnormal

60   vasoconstriction and vascular remodeling in pulmonary arteries (PAs). Various stimuli,

61   including hemodynamic stress, hypoxia, and inflammation, alter endothelial cell functions

62   and cause an imbalance in endothelial cell-derived vasoconstrictive and vasodilative factors

63   (1). Endothelin-1, prostacyclin, and nitric oxide are major regulators of vascular tone, and

64   several types of vasodilators for PAH have been developed that target these signaling

65   pathways. Although the prognosis of PAH has been remarkably improved by these

66   vasodilators (2, 3), there is still no drug that targets vascular remodeling in PAH.

67   Pulmonary arterial remodeling plays an essential role in the progression of PAH, especially

68   in the late phase of disease. Previous studies have suggested that platelet derived growth

69   factor (PDGF) and fibroblast growth factor (FGF) signaling contribute to vascular cell

70   proliferation, migration, differentiation, and apoptosis (4). Expressions of PDGF-A, PDGF-B,

71   PDGF receptor-α, and PDGF receptor-β are increased in the PAs of PAH patients

72   compared with those of healthy patients (5). Previous reports have also demonstrated

73   elevated basic FGF concentration in the plasma from PAH patients (6). FGF2 signaling

74   mediated by FGF receptor 1 (FGFR1) promotes proliferation of vascular endothelial cells (7)

75   and smooth muscle cells (8) in human PAH. Additionally, endothelial mesenchymal

76   transition (EndMT) has been suggested to contribute to the progression of occlusive

77   neointimal lesions in PAs, which is a characteristic vascular abnormality in PAH (9, 10).

78   Vascular endothelial cells acquire a mesenchymal phenotype following exposure to several

79   cytokines and growth factors, including transforming growth factor β (TGF-β), PDGF, and

80   FGF which are induced by shear stress, hypoxia, and inflammation (10). EndMT-modified

81   endothelial cells acquire additional characteristics of mesenchymal cells, and recent reports

82   have indicated a critical role of EndMT in the development of PAH-specific neointimal

83   lesions in PAs (11-13). Although both medial wall thickness and neointimal lesions in PAs

84   are common pathological findings in PAH, a greater contribution of neointimal lesions in the

85   elevation of pulmonary arterial pressure was reported in experimental PAH (14), suggesting

86   an important involvement of EndMT.

87   Nintedanib is a triple tyrosine kinase inhibitor (TKI) of PDGF, FGF, and vascular endothelial

88   growth factor (VEGF) receptors (15). A recent phase III clinical study showed that nintedanib

89   prevented both the progression of restrictive pulmonary impairment and the acute

90   exacerbation of idiopathic pulmonary fibrosis (IPF), with good tolerability (16). Thus,

91   nintedanib was approved globally for the treatment of IPF. However, the efficacy of

92   nintedanib to treat PAH by inhibiting PDGF and FGF signaling is still uncertain. Based on

93   this background information, we hypothesized that nintedanib is a novel and beneficial

94   treatment for PAH by targeting vascular remodeling including neointimal lesion and medial

95   wall thickening in PAs.

96

97   **Materials and Methods**

98   Primary human pulmonary microvascular endothelial cells (HPMVECs; product code.

99   CC-2527, lot no. 547317, 560121, and 621712) and primary human pulmonary arterial

100   smooth muscle cells (HPASMCs; product code. CC-2581, lot no. 029837, 407340, and

101   559495) were obtained from Lonza (Basel, Switzerland). All experimental and surgical

102   procedures were approved by the Institutional Committee for the Use and Care of

103   Laboratory Animals in Juntendo University (Tokyo, Japan), in accordance with the U.S.

104   National Institutes of Health Guide for the Care and Use of Laboratory Animals.

105   *EndMT of HPMVECs*

106   HPMVECs were cultured in Microvascular Endothelial Cell Growth Medium-2

107   (EGM™-2MV, Lonza). TGF-β2 (2.5 ng/mL), tumor necrosis factor (TNF)-α (2 ng/mL), and

108   interleukin (IL)-1β (4 ng/mL) were used for the induction of EndMT as previously described

109   (17). The cytokines were added to the medium with or without a 3-h preincubation with

110   nintedanib (1 μM). This concentration of nintedanib had been confirmed to have maximum

111   inhibitory effects in preliminary experiments. The expressions of von Willebrand factor

112   (vWF) and CD31 proteins, which are endothelial markers, as well as fibronectin and

113   collagen 1 proteins, which are mesenchymal markers, were analyzed at 48 h after

114   stimulation by western blotting to confirm EndMT of the HPMVECs.

115   ***Proliferation assay of HPASMCs***

116   HPASMCs were cultured in Smooth Muscle Growth Medium-2 (SmGM™-2, Lonza). The

117   proliferation of HPASMCs was evaluated using both the Cell Counting Kit-8 (CCK-8) and

118   Bromodeoxyuridine (BrdU) ELISA kit as previously described, respectively (18, 19).

119   HPASMCs were treated with multiple growth factors, specifically 5% fetal calf serum,

120   PDGF-BB (30 ng/mL), FGF2 (2 ng/mL), epidermal growth factor (EGF) (0.5 ng/mL), and

121   insulin-like growth factor-1 (IGF-1) (0.5 μg/mL) with or without imatinib (3 μM) or nintedanib

122   (0.3 μM). The viability of HPASMCs was evaluated time-dependently after stimulation. In

123   advance of this assay, we examined the concentration-dependent inhibitory effects of

124   nintedanib and imatinib, the latter of which is another TKI for PDGF signaling, on the

125   proliferation of HPASMCs induced by PDGF-BB. Based on these preliminary results, we

126   selected 0.3 μM and 3 μM of nintedanib and imatinib, respectively, as concentrations that

127   produced maximum inhibitory effects. LDH assay was also performed to assess the cell

128   toxicity of nintedanib and imatinib as previously described (20). Value of LDH in the medium

129   with nintedanib and imatinib were normalized by that in the control medium without TKI.

130   The protein expression of extracellular signal-regulated kinase (ERK)1/2 and AKT with or

131   without phosphorylation, which are downstream effectors of PDGF and FGF signaling, was

132   also evaluated by western blotting at 2 h after stimulation of the HPASMCs.

133   ***Preparation of pulmonary hypertensive rats***

134   The PAH rat model was established using Sugen 5416 (VEGF receptor-1,-2 inhibitor) and

135   chronic hypoxic exposure as previously described (14, 21). Briefly, adult male Sprague

136   Dawley rats (150 – 180 g) were injected with Sugen 5416 (20 mg/kg; Cayman Chemical Co,

137   MI) subcutaneously and exposed to hypobaric hypoxia (360 mmHg, 10% O_2) for 3 weeks.

138   After returning to normoxic conditions (760 mmHg, 21% O_2), the rats were analyzed

139   immediately [SuHx(3W) group] or were chronically treated with either vehicle (0.5%

140   hydroxyethylcellulose) [SuHx(5W) group] or nintedanib [50 mg/kg/day, SuHx(5W) + Nin

141   group] by oral gavage for 2 weeks. The dose of nintedanib was determined based on

142   previously published experiments (15). Control rats received a single vehicle injection and

143   were exposed to normoxic conditions for 5 weeks, with vehicle or nintedanib (50 mg/kg/day)

144   gavage from 3 to 5 weeks [Nx(5W)] and [Nx(5W) + Nin] groups, respectively. Hemodynamic

145   measurements were performed at 3 or 5 weeks after vehicle or Sugen 5416 injection.

146   ***Pulmonary hemodynamic measurements***

147   Pulmonary hemodynamic measurements by right heart catheterization were performed as

148   previously described (22). Briefly, all rats were anesthetized with pentobarbital sodium (30

149   mg/kg intraperitoneal). A polyvinyl catheter was inserted into the right ventricle (RV) via the

150   right jugular vein for the measurement of RV systolic pressure (RVSP) with the PowerLab

151   data acquisition system (AD Instruments, CO). Systemic systolic arterial pressure (SAP)

152   and heart rate (HR) were continuously monitored, and rats with an HR of consistently less

153   than 300 beats/min were excluded. After the hemodynamic measurements, all rats were

154   euthanized by an overdose of pentobarbital sodium, and their hearts and lungs were

155   collected for RV / left ventricle (LV) + septum weight ratio (RV/LV+S) measurements to

156   show RV hypertrophy and for histological evaluations. The right lungs were stored for

157   protein measurement, and the left lungs were inflated with 10% buffered formalin at a

158   constant pressure of 20 cm H_2O for histological analyses. Fixation was allowed to proceed

159   overnight.

160   ***Morphological analysis of PAs***

161   The inflated and fixed left lungs were embedded in paraffin. All sections were cut at 5-μm

162   thickness and were stained with elastic Van Gieson stain. A quantitative analysis of PA

163   luminal obstruction was performed as described previously with minor modifications (14).

164   We counted between 100 and 200 small PAs [outer diameter (OD) < 200 μm] per whole left

165   lobe at ×400 magnification using an image analysis system (KS400; Carl Zeiss Imaging

166   Solutions, Germany) in a blind manner. The medial-wall thickness was measured for the

167   arteries with an OD between 50 and 200 µm. The distance between the internal and

168   external elastic laminae was expressed as the medial thickness/OD. Vessels with an OD <

169   50 µm were used for the assessment of occlusive neointimal lesions and were scored as

170   follows: no evidence of occlusive neointimal formation (grade 0), partial luminal occlusion (≤

171   50%; grade 1), and severe luminal occlusion (> 50%; grade 2).

172   ***Immunohistochemistry of PAs***

173   After deparaffinization with xylene, rehydration, and antigen retrieval by heating in citrate

174   buffer (pH 6), immunohistochemistry was performed with an anti-FGFR1 (phospho Y654)

175   antibody (ab59194, Abcam, Cambridge, UK), anti-PDGF receptor-β (phospho Y1020)

176   antibody (ab16868, Abcam, Cambridge, UK). The signals were detected using

177   VECTASTAIN® elite ABC rabbit, mouse and goat IgG kits (#PK-6101, 6102, 6105, Vector

178   Laboratories, CA). In each whole left lobe, 100 arteries across serial sections were

179   examined to evaluate the expression of each receptor.

180   ***Expression of Twist1 in rat lung tissues***

181   The expression of Twist1 protein, which is an EndMT-related transcription factor (11), was

182   evaluated by western blotting in lung tissues from Nx(5W), SuHx(5W), and SuHx(5W) + Nin

183   groups to assess the contribution of EndMT in the vascular remodeling of PAs in rat PAH

184   and to assess the anti-EndMT effect of nintedanib.

185   ***Western blotting analysis***

186   HPASMCs, HPMVECs, and lung tissues were lysed in radioimmunoprecipitation assay

187   (RIPA) buffer containing protease and phosphatase inhibitors, and the lysates were

188   subjected to western blotting, as described previously (23). Transferred membranes were

189   allowed to react with anti-vWF polyclonal antibody (1:1,000; sc14014, Santa Cruz

190   Biotechnology), anti-CD31 monoclonal antibody (1:2,000; bba7, R&D Systems, MN),

191   anti-fibronectin monoclonal antibody (1:2,000; sc59826, Santa Cruz Biotechnology),

192   anti-Collagen 1 polyclonal antibody (1:1,000; ab34710, Abcam), anti-p44/42 MAPK (Erk1/2)

193   Antibody (1:2,000; #9102, Cell Signaling Technology), anti-Phospho-p44/42 MAPK (Erk1/2)

194   (Thr202/Tyr204) Antibody (1:2,000; #9101, Cell Signaling Technology), anti-AKT polyclonal

195   antibody (1:2,000; #9272, Cell Signaling Technology), anti-phospho-AKT (Ser473)

196   polyclonal antibody (1:2,000; #9271, Cell Signaling Technology), anti-Twist1 polyclonal

197   antibody (1:1000; ab50581, Abcam), or anti-β-actin monoclonal antibody (1:10,000; A5441,

198   Sigma, MO). Western blot signals were acquired using a Fuji ImageQuant™ LAS-4000

199   fluorescence imager and quantified using the Multi Gauge image analysis software (Fujifilm

200   Corporation, Tokyo, Japan). The densitometric signal of each protein was normalized to that

201   of β-actin.

202   ***Statistical analysis***

203   Data are presented as means ± SE. Statistical analysis was performed using one-way

204   ANOVA (Prism 6; GraphPad Software, La Jolla, CA, USA). Differences were considered

205   significant at $P < 0.05$.

206

207   **Results**

208   ***Inhibitory effect of nintedanib on EndMT of HPMVECs***

209   We confirmed decreased expression of vWF and CD31 proteins and increased expression

210   of fibronectin and collagen 1 proteins by western blotting. Nintedanib attenuated the

211   upregulation of mesenchymal markers in the stimulated HPMVECs, but did not prevent the

212   downregulation of endothelial markers (Figure 1A, B). After stimulation with TGF-β2, TNF-α,

213   and IL-1β, the morphology of HPMVECs changed from a cobblestone to spindle-shaped

214   morphology, and nintedanib tended to prevent its change. (Figure 1C).

215   ***Inhibitory effect of nintedanib on proliferation of HPASMCs***

216   The proliferation of HPASMCs induced by multiple growth factors (PDGF-BB, FGF2, EGF,

217   and IGF) was significantly greater than that without stimulation in CCK-8 and BrdU assays,

218   and nintedanib significantly inhibited this proliferation at 24 and 48 h after stimulation.

219   Moreover, the inhibitory effect of nintedanib was significantly greater than that of imatinib at

220   48 h after stimulation in CCK-8 assay (Figure 2A, 2B). Values of LDH in the medium after

221   treatment with imatinib and nintedanib were similar between all groups (Figure 2C). The

222   phosphorylation of ERK1/2 and AKT was increased in the HPASMCs stimulated with

223   multiple growth factors, and nintedanib remarkably prevented these phosphorylations. This

224   preventive effect of nintedanib was significantly greater than that of imatinib on the

225   phosphorylated AKT (Figure 2D).

226   ***Chronic treatment with nintedanib in PAH rats***

227   The rats were divided into 5 groups as follows: 5-week normoxia + vehicle group [Nx(5W)],

228   5-week normoxia + nintedanib group [Nx(5W) + Nin)], Sugen 5416 + hypoxia + vehicle

229   group [SuHx(3W) and SuHx(5W)], and Sugen 5416 + hypoxia + nintedanib group

230   [SuHx(5W) + Nin] (Figure 3A). Three weeks after Sugen 5416 injection and hypoxic

231   exposure, the RVSP and RV/LV+S were already higher in the SuHx(3W) group (81.3 ± 2.7

232   mmHg and 0.688 ± 0.034, respectively) than in the Nx(5W) group (22.4 ± 1.1 mmHg and

233   0.296 ± 0.014, respectively). After 2 weeks of treatment with nintedanib [SuHx(5W) + Nin],

234   the RVSP and RV/LV+S were significantly reduced (50.4 ± 7.2 mmHg and 0.546 ± 0.029,

235   respectively) compared with those of the SuHx(5W) group (81.8 ± 6.6 mmHg and $0.728 \pm$

236   0.023, respectively). Treatment with nintedanib under normoxic condition [Nx(5W) + Nin]

237   caused no effect on pulmonary hemodynamics (Figure 3B). Chronic treatment with

238   nintedanib also did not affect the systemic SAP, HR, or body weight (Figure 3C). The values

239   of RVSP and RV/LV+S in the SuHx(5W) rats are consistent with those of a previous study

240   (14).

241   The medial wall thickness of PAs (50 to 200 μm OD) in the [SuHx(5W)+Nin] group was

242   significantly reduced compared to that in the SuHx(3W) and SuHx(5W) groups. The grade 1

243   and grade 2 neointimal occlusive lesions in the small PAs (< 50 μm OD) were also

244   significantly lower in [SuHx(5W) + Nin] than in SuHx(3W) and in SuHx(5W). Although the

245   medial wall thickening and grade 1 neointimal occlusive lesions were reversed by treatment

246   with nintedanib compared with the SuHx(3W) values, nintedanib treatment lessened, but did

247   not reverse, the development of grade 2 neointimal occlusive lesions (Figure 4A, B). Both

248   medial wall thickness and neointimal lesions with the severe PH group tended to be

249   progressive compared to those of the less severe PH group.

250   ***Phosphorylation of FGF and PDGF receptors in PAs***

251   The expression of phosphorylated FGFR1 and PDGF receptor-β were significantly

252   increased not only in PAs with medial wall thickening (OD 50–200 μm), but also in PAs with

253   occlusive neointimal lesions (OD < 50 μm), in contrast to the low levels in the PAs of Nx(5W)

254   lungs. The phosphorylation of FGFR1 and PDGF receptor-β in PAs was significantly

255 decreased by 2-week treatment with nintedanib [SuHx(5W) + Nin] (Figure 5A, B).

256 ***Expression of Twist1 in rat lung tissue***

257 The expression of Twist1 protein by western blotting was significantly augmented in lung

258 tissue from SuHx(5W) rats compared with that from Nx(5W) rats, and nintedanib remarkably

259 reduced this augmented expression (Figure 6).

260

261 **Discussion**

262 This report assessed the beneficial effect of nintedanib for PAH both *in vitro* and *in vivo*.

263 Nintedanib attenuated the progression of EndMT in HPMVECs and inhibited the

264 proliferation of HPASMCs *in vitro*. In addition, we demonstrated that phosphorylated PDGF

265 and FGF receptors were increased in vascular occlusive neointimal lesions and the

266 thickening medial wall in PAH rats. Two-week treatment of PAH rats with nintedanib

267 significantly ameliorated pulmonary hemodynamics accompanied with improved vascular

268 remodeling of PAs.

269 ***Mechanism of pulmonary arterial remodeling in PAH***

270 Medial wall thickening and occlusive neointimal lesion of PAs are common pathological

271 findings in PAH. In the remodeling process of PAs in PAH, medial wall thickening driven by

272 proliferation and hypertrophy of smooth muscle cells occurs early in disease progression.

273   Moreover, the contribution of functional changes in smooth muscle cells of different

274   phenotypes occurs particularly in the establish phase (24). On the other hand, a greater

275   contribution of neointimal lesions than of medial wall thickness in the development of PAH

276   was shown in an experimental model (14), and the role of EndMT in the progression of

277   neointimal lesions has been recently suggested (10-13).

278   The essential role of EndMT in the pathogenesis of various cardiovascular diseases and

279   PAH has been recently demonstrated (25). Occlusive neointimal lesions in small PAs,

280   including plexiform lesions, are characteristic in PAH, and the proliferative cells that

281   comprise these PAH-specific neointimal lesions have both endothelial and mesenchymal

282   phenotypes (9, 11). Inducers, such as a hemodynamic stress, mechanical injury, hypoxia,

283   and inflammation, upregulate several growth factors and cytokines, including PDGF, FGF,

284   and TGF-β, which play important roles in the progression of EndMT (26, 27). Endothelial

285   cells lose their intercellular adhesion after exposure to these stimuli, and subsequently

286   change from a cobblestone to spindle-shaped morphology. EndMT-induced endothelial

287   cells express both endothelial and mesenchymal markers, and acquire further capacity to

288   proliferate, migrate, and avoid apoptosis (10). In a PAH model, both endothelial and

289   mesenchymal markers were seen by immunohistochemistry in neointimal lesions of small

290   PAs (12). Recent reports also have shown that green fluorescent protein (GFP)-labeled

291   endothelial cells in mice were transformed by Sugen 5416 injection and chronic hypoxic

292   exposure to a mesenchymal phenotype with high proliferative and migratory abilities (13). In

293   human PAH, Ranchoux *et al*. demonstrated by electron microscopy that caveolae, which

294   are characteristic of vascular endothelial cells, and dense bodies, which are dominant in

295   vascular smooth muscle cells, were present in the same cells comprising occlusive

296   neointimal lesions. Moreover, the expression of Twist1, a transcription factor associated with

297   EndMT, was higher in human PAH lung than in normal human lung (11). These data

298   indicate a critical contribution of EndMT in the progression of neointimal lesions in PAH.

299   ***Tyrosine kinase inhibitors for PAH***

300   Imatinib is a TKI for Bcr-Abl, c-Kit, c-Abl, and PDGF receptor signaling, and has been used

301   for the treatment of chronic myelogenous leukemia and gastrointestinal stromal tumors (28).

302   Imatinib was also expected to be a novel anti-vascular treatment for PAH due to its inhibitory

303   effect on PDGF receptor. Imatinib was shown to inhibit the proliferation of HPASMCs from

304   PAs in human PAH (29), and long-term treatment with imatinib prevented the development

305   of chronic hypoxia- and monocrotaline-induced pulmonary hypertension in rats (30, 31) .

306   Furthermore, imatinib combined with various vasodilators significantly improved 6-minute

307   walking distance and pulmonary vascular resistance in human patients, and a phase III

308   clinical study of imatinib for PAH was implemented (32). However, imatinib did not receive

309 final approval for PAH because of its serious adverse effects. Dasatinib, a TKI for Bcr-Abl,

310 c-kit, Src family and PDGF receptor signaling, has been used also to treat chronic

311 myelogenous leukemia. Importantly, dasatinib-induced pulmonary hypertension has been

312 previously reported, suggesting specific toxicity of dasatinib on pulmonary vessels (33, 34).

313 Nintedanib is a TKI for PDGF, FGF, and VEGF receptors. FGFR1, 2, and 3; PDGF

314 receptor-α and -β; and VEGF receptor-1, -2, and -3 are receptors that are targeted by

315 nintedanib (35). Nintedanib was originally developed for the treatment of malignancies as an

316 agent to inhibit angiogenesis, cell proliferation, and migration (36). Nintedanib also reduced

317 the mRNA and protein expression of extracellular matrix components in fibroblasts from

318 human IPF (37), indicating the ability of nintedanib to treat IPF. Additionally, a recent phase

319 III clinical study for human IPF showed beneficial effects of nintedanib in improving forced

320 vital capacity and reducing the incidence of acute exacerbations. Diarrhea and liver

321 dysfunction are major adverse effects of nintedanib, but these events were generally well

322 tolerated (16). Hence, nintedanib has been approved globally for the treatment of IPF. In

323 contrast to dasatinib, the results from the phase III study and postmarketing surveillance

324 revealed no evidence to warrant elevating the risk of pulmonary hypertension by nintedanib.

325 Based on this background, we hypothesized that nintedanib was a novel and tolerable

326 treatment for PAH because of its anti-vascular remodeling via inhibition of PDGF and FGF

327   signaling.

328   ***Effect of nintedanib in vitro***

329   In this study, nintedanib significantly prevented the increased expression of mesenchymal

330   markers in EndMT-induced HPMVECs. A recent report showed that nintedanib reduced

331   TGF-β signaling via inhibition of SMAD3 and p38 MAPK pathways (37). TGF-β signaling is

332   considered a major regulator of EndMT, suggesting that the inhibition of TGF-β signaling is

333   one of the mechanisms of the anti-EndMT effect by nintedanib. Moreover, previous reports

334   showed that PDGF and FGF enhanced signaling of p38/AKT and PI3K/AKT pathways.

335   Increased p38/PI3K/AKT signaling affected the expression of endothelial markers involving

336   vWF and CD31 via transcription factors involving Twist1 (25). These data suggest that

337   nintedanib can also regulate EndMT via inhibition of PDGF/FGF receptor tyrosine kinase

338   activity in addition to TGF-β signaling. On the other hand, the reduced expression of

339   endothelial markers was not restored after treatment with nintedanib. HPMVECs were

340   pretreated with nintedanib before induction of EndMT in this study. Blockade of VEGF

341   signaling by nintedanib may disrupt the maintenance of endothelial cell characteristics,

342   because VEGF signaling generally plays an endothelial protective role (38).

343   In HPASMCs, nintedanib also significantly prevented the proliferation induced by multiple

344   growth factors, and the inhibitory effect of nintedanib was significantly greater than that of

345 imatinib after co-stimulation with multiple growth factors. The LDH assay showed no

346 difference even after treatment with nintedanib, suggesting no toxicity of nintedanib for

347 HPASMCs. ERK1/2 and AKT, which are downstream effectors of PDGF and FGF signaling,

348 play roles in the regulation of vascular smooth muscle cell proliferation and apoptosis.

349 Nintedanib also remarkably reduced the phosphorylation of ERK1/2 and AKT after

350 co-stimulation, and this inhibitory effect of nintedanib was greater than that of imatinib.

351 These *in vitro* results suggest a beneficial, anti-remodeling effect of nintedanib in the intima

352 and media of PAs in PAH.

353 ***Effect of nintedanib in vivo***

354 Classical animal models of pulmonary hypertension that are induced by chronic hypoxic

355 exposure and monocrotaline have no neointimal lesions in the small PAs. Hence, these

356 models were considered inappropriate for the study of PAH. In the present study, we used

357 SuHx-PAH rats, which have neointimal lesions similar to those in human PAH (39), to

358 evaluate the effect of nintedanib. Toba *et al*. provided a detailed evaluation of the time

359 course progression of vascular remodeling in the SuHx-PAH rat (14). They observed

360 thickened medial walls and neointimal lesions in PAs from 3 to 5 weeks, whereas fibrotic

361 vasculopathy involving plexiform lesions progressed 8 weeks following injection of Sugen

362 5416. Although the medial wall thickness decreased to a normal range during the late phase

363   of PAH even with an elevated RVSP, the increased density of severely occlusive PAs was

364   obviously correlated with RVSP elevation. Thus, the authors concluded that the contribution

365   of medial wall thickness was transient in the early phase of PAH, and the role of neointimal

366   lesions in the small PAs seemed to be greater in the progression of disease. Whereas

367   neointimal lesions are an important therapeutic target for the treatment of PAH, vascular

368   lesions with substantial fibrosis are generally considered refractory to treatment (40).

369   Therefore, we tested the anti-remodeling effect of nintedanib from 3 to 5 weeks in this study,

370   targeting non-plexiform cellular neointimal vascular lesions. The phosphorylation of PDGF

371   and FGF receptors significantly increased in the proliferative neointimal lesions and medial

372   walls in the PAH rat, indicating that these PAH-specific neointimal lesions could be a major

373   therapeutic target of nintedanib. In fact, nintedanib treatment from 3 to 5 weeks significantly

374   reduced the expression of those receptors and prevented the progression of neointimal

375   lesions, resulting in improved pulmonary hemodynamics in the PAH rats. Furthermore, we

376   showed increased expression of Twist1 protein in the lung tissue from SuHx-PAH rats.

377   Twist1 enhances the expression of TGF-β receptor and phosphorylation of SMAD2, and can

378   lead to EndMT in PA endothelial cells (41). Chronic nintedanib significantly reduced Twist1

379   protein expression in this study. These findings indicate not only the contribution of EndMT

380   in the development of proliferative occlusive neointimal lesions in PAH rats, but also the

381   anti-EndMT effects of nintedanib. Additionally, it has been reported that BIBF1000, a

382   structural precursor of nintedanib, did not disturb RV function in rats subjected to

383   mechanical pressure overload by pulmonary artery-banding (42). Another recent study also

384   showed that less dilatation, decreased fibrosis and hypertrophy of right ventricle after

385   chronic treatment with nintedanib in Su/Hx-PAH rat by echocardiography and histological

386   analysis (43), suggesting no cardiac toxicity of nintedanib.

387   A recently published study demonstrated that nintedanib had no therapeutic effect on rat

388   and human PAH (44), which contradicted our results. Several factors could explain the

389   discrepancy between the studies. For instance, rat strain that were used for experimental

390   PAH were different. A previous report has shown that the severity of the response to

391   Sugen5416 with hypoxic exposure was remarkably different between rat strains (45).

392   Actually, the RVSP of SuHx PAH in Wistar-Kyoto rats was obviously lower in a recent study

393   than in this study. Therefore, the response to nintedanib also may be dissimilar between

394   strains. As another factor, muscularization of the small PAs was evaluated to assess the

395   effect of nintedanib in a recent study. Such measurement is common for hypoxic or

396   monocrotaline-induced pulmonary hypertension models that have no neointimal lesions, but

397   it is not appropriate for the SuHx PAH rat which has neointimal lesions in the small PAs. In

398   addition, pathological images of small PAs were not shown in that study; thus, it is unclear

399   which parts of the small PAs were evaluated. Furthermore, the delivery route of nintedanib

400   to the rat was not mentioned. Thus, the possibility remain that differences in the

401   administration route of nintedanib may be the cause of the contradictory results. In contrast,

402   Huang et al. reported that chronic treatment with nintedanib reduced pulmonary vascular

403   remodeling in the Fos-related antigen-2 mouse model of systemic sclerosis (46), which was

404   supportive of our results. On the other hand, another more recent study showed that chronic

405   treatment with nintedanib of established late-phase PAH, from 8 to 11 weeks, did not

406   improved pulmonary hemodynamics and vascular remodeling in SuHx rats (43). The results

407   of these recent studies of established animal and human PAH suggest that the therapeutic

408   power of nintedanib may be limited at least in advanced stages of PAH. Although the

409   efficacy of nintedanib for mild to moderate PAH is still uncertain, the therapeutic benefit of

410   nintedanib may rest with its ability to augment the effect of other vasodilators or to prevent

411   the progression of PAH.

412   **Limitations**

413   Our study has a few limitations. First, we have not yet assessed the phenotype of

414   HPASMCs after stimulation; investigations into the effect of nintedanib on the functional

415   changes in HPASMCs may bring further beneficial information. Second, while HPASMC

416   used in this study is mainly isolated from the proximal PA, contribution of small distal PA is

417   greater than that of large proximal PA in the disease progression of PAH. Thus, data would

418   be more useful by using HPASMC isolated from only small distal PA. Third, the mechanism

419   of the inhibitory effect of nintedanib on EndMT progression is still unclear. We induced

420   EndMT in HPMVECs by using three different inducers simultaneously; nintedanib could

421   have inhibited all three signaling pathways. The inhibitory mechanism was probably very

422   complex and beyond the scope of the current study. Fourth, higher concentrations or longer

423   regimens of nintedanib treatment for PAH in the rat have not yet been evaluated. Further

424   experiments are necessary in the future to evaluate these limitations of our study.

425   **Conclusion**

426   In conclusion, we have shown the beneficial effects of nintedanib for PAH *in vitro* and *in*

427   *vivo*. Chronic treatment with nintedanib reversed the elevated pulmonary arterial pressure in

428   the PAH rat via anti-EndMT effects in HPMVECs and anti-proliferative effects in HPASMCs.

429   Moreover, an expanded indication of nintedanib for the treatment of PAH would be

430   advantageous, since nintedanib has been approved already for the treatment of other

431   human diseases with good tolerability. Although further investigations are necessary, the

432   results of this study indicate that nintedanib may be a novel additional option for the

433   treatment of human PAH, with an anti-vascular remodeling effect.

434

444   **References**

445   1.   Lai YC, Potoka KC, Champion HC, Mora AL, Gladwin MT. Pulmonary arterial

446   hypertension: the clinical syndrome. Circ Res. 2014;115(1):115-30.

447   2.   Hurdman J, Condliffe R, Elliot CA, Davies C, Hill C, Wild JM, et al. ASPIRE

448   registry: assessing the Spectrum of Pulmonary hypertension Identified at a REferral centre.

449   Eur Respir J. 2012;39(4):945-55.

450   3.   Frost AE, Badesch DB, Miller DP, Benza RL, Meltzer LA, McGoon MD. Evaluation

451   of the predictive value of a clinical worsening definition using 2-year outcomes in patients

452   with pulmonary arterial hypertension: a REVEAL Registry analysis. Chest.

453   2013;144(5):1521-9.

454   4.   Noskovicova N, Petrek M, Eickelberg O, Heinzelmann K. Platelet-derived growth

455   factor signaling in the lung. From lung development and disease to clinical studies. Am J

456   Respir Cell Mol Biol. 2015;52(3):263-84.

457   5.   Perros F, Montani D, Dorfmuller P, Durand-Gasselin I, Tcherakian C, Le Pavec J,

458   et al. Platelet-derived growth factor expression and function in idiopathic pulmonary arterial

459   hypertension. Am J Respir Crit Care Med. 2008;178(1):81-8.

460   6.   Benisty JI, McLaughlin VV, Landzberg MJ, Rich JD, Newburger JW, Rich S, et al.

461   Elevated basic fibroblast growth factor levels in patients with pulmonary arterial

462   hypertension. Chest. 2004;126(4):1255-61.

463   7.   Tu L, Dewachter L, Gore B, Fadel E, Dartevelle P, Simonneau G, et al. Autocrine

464   fibroblast growth factor-2 signaling contributes to altered endothelial phenotype in

465   pulmonary hypertension. Am J Respir Cell Mol Biol. 2011;45(2):311-22.

466   8.   Izikki M, Guignabert C, Fadel E, Humbert M, Tu L, Zadigue P, et al.

467   Endothelial-derived FGF2 contributes to the progression of pulmonary hypertension in

468   humans and rodents. J Clin Invest. 2009;119(3):512-23.

469   9.   Tuder RM, Groves B, Badesch DB, Voelkel NF. Exuberant endothelial cell growth

470   and elements of inflammation are present in plexiform lesions of pulmonary hypertension.

471   The American journal of pathology. 1994;144(2):275-85.

472   10.   Arciniegas E, Frid MG, Douglas IS, Stenmark KR. Perspectives on

473   endothelial-to-mesenchymal transition: potential contribution to vascular remodeling in

474   chronic pulmonary hypertension. Am J Physiol Lung Cell Mol Physiol. 2007;293(1):L1-8.

475   11.   Ranchoux B, Antigny F, Rucker-Martin C, Hautefort A, Pechoux C, Bogaard HJ, et

476   al. Endothelial-to-mesenchymal transition in pulmonary hypertension. Circulation.

477   2015;131(11):1006-18.

478   12.   Good RB, Gilbane AJ, Trinder SL, Denton CP, Coghlan G, Abraham DJ, et al.

479   Endothelial to Mesenchymal Transition Contributes to Endothelial Dysfunction in Pulmonary

480   Arterial Hypertension. The American journal of pathology. 2015;185(7):1850-8.

481   13.   Suzuki T, Carrier EJ, Talati MH, Rathinasabapathy A, Chen X, Nishimura R, et al.

482   Isolation and characterization of endothelial-to-mesenchymal transition cells in pulmonary

483   arterial hypertension. Am J Physiol Lung Cell Mol Physiol. 2018;314(1):L118-L26.

484   14.   Toba M, Alzoubi A, O'Neill KD, Gairhe S, Matsumoto Y, Oshima K, et al. Temporal

485   hemodynamic and histological progression in Sugen5416/hypoxia/normoxia-exposed

486   pulmonary arterial hypertensive rats. Am J Physiol Heart Circ Physiol.

487   2014;306(2):H243-50.

488   15.   Wollin L, Wex E, Pautsch A, Schnapp G, Hostettler KE, Stowasser S, et al. Mode

489   of action of nintedanib in the treatment of idiopathic pulmonary fibrosis. Eur Respir J.

490   2015;45(5):1434-45.

491   16.   Richeldi L, du Bois RM, Raghu G, Azuma A, Brown KK, Costabel U, et al. Efficacy

492   and safety of nintedanib in idiopathic pulmonary fibrosis. N Engl J Med.

493   2014;370(22):2071-82.

494   17.   Nagai T, Kanasaki M, Srivastava SP, Nakamura Y, Ishigaki Y, Kitada M, et al.

495   N-acetyl-seryl-aspartyl-lysyl-proline inhibits diabetes-associated kidney fibrosis and

496   endothelial-mesenchymal transition. Biomed Res Int. 2014;2014:696475.

497   18.   Zhou H, Wang Y, Zhou Q, Wu B, Wang A, Jiang W, et al. Down-Regulation of

498   Protein Kinase C-epsilon by Prolonged Incubation with PMA Inhibits the Proliferation of

499   Vascular Smooth Muscle Cells. Cell Physiol Biochem. 2016;40(1-2):379-90.

500   19.   Muir D, Varon S, Manthorpe M. An enzyme-linked immunosorbent assay for

501   bromodeoxyuridine incorporation using fixed microcultures. Anal Biochem.

502   1990;185(2):377-82.

503   20.   Wakatsuki S, Furuno A, Ohshima M, Araki T. Oxidative stress-dependent

504   phosphorylation activates ZNRF1 to induce neuronal/axonal degeneration. J Cell Biol.

505   2015;211(4):881-96.

506   21.   Sakao S, Tatsumi K. The effects of antiangiogenic compound SU5416 in a rat

507   model of pulmonary arterial hypertension. Respiration. 2011;81(3):253-61.

508   22.   Kuriyama S, Morio Y, Toba M, Nagaoka T, Takahashi F, Iwakami S, et al.

509   Genistein attenuates hypoxic pulmonary hypertension via enhanced nitric oxide signaling

510   and the erythropoietin system. Am J Physiol Lung Cell Mol Physiol.

511   2014;306(11):L996-L1005.

512   23.   Pullamsetti SS, Berghausen EM, Dabral S, Tretyn A, Butrous E, Savai R, et al.

513   Role of Src tyrosine kinases in experimental pulmonary hypertension. Arteriosclerosis,

514   thrombosis, and vascular biology. 2012;32(6):1354-65.

515   24.   Stenmark KR, Frid MG, Graham BB, Tuder RM. Dynamic and diverse changes in

516   the functional properties of vascular smooth muscle cells in pulmonary hypertension.

517   Cardiovasc Res. 2018;114(4):551-64.

518   25.   Jackson AO, Zhang J, Jiang Z, Yin K. Endothelial-to-mesenchymal transition: A

519   novel therapeutic target for cardiovascular diseases. Trends Cardiovasc Med.

520   2017;27(6):383-93.

521   26.   Li Z, Jimenez SA. Protein kinase Cdelta and c-Abl kinase are required for

522   transforming growth factor beta induction of endothelial-mesenchymal transition in vitro.

523   Arthritis Rheum. 2011;63(8):2473-83.

524   27.   Song S, Zhang M, Yi Z, Zhang H, Shen T, Yu X, et al. The role of

525   PDGF-B/TGF-beta1/neprilysin network in regulating endothelial-to-mesenchymal transition

526   in pulmonary artery remodeling. Cell Signal. 2016;28(10):1489-501.

527   28.   Peng B, Lloyd P, Schran H. Clinical pharmacokinetics of imatinib. Clinical

528   pharmacokinetics. 2005;44(9):879-94.

529   29.   Nakamura K, Akagi S, Ogawa A, Kusano KF, Matsubara H, Miura D, et al.

530   Pro-apoptotic effects of imatinib on PDGF-stimulated pulmonary artery smooth muscle cells

531   from patients with idiopathic pulmonary arterial hypertension. Int J Cardiol.

532   2012;159(2):100-6.

533   30.   Ciuclan L, Hussey MJ, Burton V, Good R, Duggan N, Beach S, et al. Imatinib

534 attenuates hypoxia-induced pulmonary arterial hypertension pathology via reduction in

535 5-hydroxytryptamine through inhibition of tryptophan hydroxylase 1 expression. Am J Respir

536 Crit Care Med. 2013;187(1):78-89.

537 31.   Pankey EA, Thammasiboon S, Lasker GF, Baber S, Lasky JA, Kadowitz PJ.

538 Imatinib attenuates monocrotaline pulmonary hypertension and has potent vasodilator

539 activity in pulmonary and systemic vascular beds in the rat. Am J Physiol Heart Circ Physiol.

540 2013;305(9):H1288-96.

541 32.   Hoeper MM, Barst RJ, Bourge RC, Feldman J, Frost AE, Galie N, et al. Imatinib

542 mesylate as add-on therapy for pulmonary arterial hypertension: results of the randomized

543 IMPRES study. Circulation. 2013;127(10):1128-38.

544 33.   Montani D, Bergot E, Gunther S, Savale L, Bergeron A, Bourdin A, et al.

545 Pulmonary arterial hypertension in patients treated by dasatinib. Circulation.

546 2012;125(17):2128-37.

547 34.   Guignabert C, Phan C, Seferian A, Huertas A, Tu L, Thuillet R, et al. Dasatinib

548 induces lung vascular toxicity and predisposes to pulmonary hypertension. J Clin Invest.

549 2016;126(9):3207-18.

550 35.   Inomata M, Nishioka Y, Azuma A. Nintedanib: evidence for its therapeutic potential

551 in idiopathic pulmonary fibrosis. Core Evid. 2015;10:89-98.

552 36.   Caglevic C, Grassi M, Raez L, Listi A, Giallombardo M, Bustamante E, et al.

553 Nintedanib in non-small cell lung cancer: from preclinical to approval. Ther Adv Respir Dis.

554 2015;9(4):164-72.

555 37.   Rangarajan S, Kurundkar A, Kurundkar D, Bernard K, Sanders YY, Ding Q, et al.

556 Novel Mechanisms for the Antifibrotic Action of Nintedanib. Am J Respir Cell Mol Biol.

557 2016;54(1):51-9.

558 38.   Voelkel NF, Gomez-Arroyo J. The role of vascular endothelial growth factor in

559 pulmonary arterial hypertension. The angiogenesis paradox. Am J Respir Cell Mol Biol.

560 2014;51(4):474-84.

561 39.   Abe K, Toba M, Alzoubi A, Ito M, Fagan KA, Cool CD, et al. Formation of plexiform

562 lesions in experimental severe pulmonary arterial hypertension. Circulation.

563 2010;121(25):2747-54.

564 40.   Sakao S, Tatsumi K, Voelkel NF. Reversible or irreversible remodeling in

565 pulmonary arterial hypertension. Am J Respir Cell Mol Biol. 2010;43(6):629-34.

566 41.   Kwapiszewska G, Crnkovic S, Stenmark KR. A Twist on Pulmonary Vascular

567 Remodeling: Endothelial to Mesenchymal Transition? Am J Respir Cell Mol Biol.

568 2018;58(2):140-1.

569 42.   de Raaf MA, Herrmann FE, Schalij I, de Man FS, Vonk-Noordegraaf A, Guignabert

570 C, et al. Tyrosine kinase inhibitor BIBF1000 does not hamper right ventricular pressure

571 adaptation in rats. Am J Physiol Heart Circ Physiol. 2016;311(3):H604-12.

572 43. Rol N, de Raaf MA, Sun X, Kuiper VP, da Silva Goncalves Bos D, Happe C, et al.

573 Nintedanib improves cardiac fibrosis but leaves pulmonary vascular remodeling unaltered in

574 experimental pulmonary hypertension. Cardiovasc Res. 2018.

575 44. Richter MJ, Ewert J, Grimminger F, Ghofrani HA, Kojonazarov B, Petrovic A, et al.

576 Nintedanib in Severe Pulmonary Arterial Hypertension. Am J Respir Crit Care Med. 2018.

577 45. Jiang B, Deng Y, Suen C, Taha M, Chaudhary KR, Courtman DW, et al. Marked

578 Strain-Specific Differences in the SU5416 Rat Model of Severe Pulmonary Arterial

579 Hypertension. Am J Respir Cell Mol Biol. 2016;54(4):461-8.

580 46. Huang J, Maier C, Zhang Y, Soare A, Dees C, Beyer C, et al. Nintedanib inhibits

581 macrophage activation and ameliorates vascular and fibrotic manifestations in the Fra2

582 mouse model of systemic sclerosis. Ann Rheum Dis. 2017;76(11):1941-8.

583

584

585   **Figure legends.**

586   Figure 1. Inhibitory effect of nintedanib on endothelial mesenchymal transition of human

587   pulmonary microvascular endothelial cells.

588   Inhibitory effect of nintedanib (Nin) on endothelial–mesenchymal transition (EndMT) of

589   human pulmonary microvascular endothelial cells (HPMVEC). EndMT was induced by

590   stimulation with TGF-β2, TNF-α, and IL-1β (Stimu). Unstimulated cells are denoted as

591   CON. Expression of (A) von Willebrand factor (vWF) and CD31 proteins, which are

592   endothelial markers, and (B) fibronectin and collagen 1 proteins, which are mesenchymal

593   markers. * $p<0.01$ vs. CON. # $p<0.001$ vs. Stimu. (C) Representative morphology of

594   HPMVECs in Con, Stimu, and Stimu+Nin condition.

595   .

596

597   Figure 2. Inhibitory effect of nintedanib on proliferation of human pulmonary arterial smooth

598   muscle cells.

599   (A) Inhibitory effect of nintedanib (Nin) and imatinib (Ima) on proliferation of human

600   pulmonary arterial smooth muscle cells (HPASMCs) using the CCK-8 assay. Cell viability of

601   HPASMC was assessed at 0, 12, 24, and 48 h after stimulation with multiple growth factors

602   (MGF, platelet derived growth factor-BB + fibroblast growth factor 2 + epidermal growth

603   factor + insulin-like growth factor-1). Con: control HPASMC without MGF stimulation. Values

604   are means ± SE (n=5). * p<0.001 MGF vs. Con. § p<0.01 MGF vs. MGF + Ima. # p<0.01

605   MGF vs. MGF + Nin. ¶ p<0.05 MGF + Nin vs. MGF + Ima. (B) Inhibitory effect of Nin and

606   Ima on proliferation of HPASMC using the BrdU assay. Cell viability of HPASMC was

607   assessed at 24 and 48 h after stimulation with MGF. ** p<0.001. Plotted values are means ±

608   SE (n=6). (C) Cell toxicity of Nin and Ima on HPASMC using the LDH assay. Values of LDH

609   were assessed at 24 and 48 h after treatment of Nin and Ima. Value of LDH in the medium

610   with Nin and Ima were normalized by that in the control medium. Plotted values are means ±

611   SE (n=6). (D) Expressions of ERK1/2, phosphorylated ERK1/2 (pERK1/2), AKT, and

612   phosphorylated AKT (pAKT) protein with or without Nin or Ima by western blotting.

613   Representative blots are shown in the upper panels. Densitometric signals of the

614   phosphorylated protein were normalized to the corresponding non-phosphorylated protein.

615   Plotted values are means ± SE (n=6). * p<0.01. ** p<0.001. n.s. not significantly.

616

617   Figure 3. Effect of chronic nintedanib for the development of pulmonary arterial hypertension

618   in rat.

619   (A) *In vivo* experimental timeline. Outcomes include measurement of pulmonary

620   hemodynamics and right ventricle hypertrophy, and/or morphometric analysis of pulmonary

621 arteries. Nx: control rat with normoxic condition. SuHx: single injection of Sugen 5416 with

622 chronic hypoxic exposure. W: week. (B) Chronic effect of nintedanib in Su/Hx rat.

623 Examinations of right ventricle systolic pressure (RVSP) and right ventricle weight / (left

624 ventricle and septal weight) ratio (RV/LV+S) in normoxic rats at 5 weeks [Nx(5W)], Nx rat

625 with nintedanib treatment from weeks 3 to 5 [Nx(5W) + Nin], Su/Hx rat at 3 weeks

626 [SuHx(3W)] or at 5 weeks [SuHx(5W)] after Sugen 5416 injection, and SuHx rats with

627 nintedanib treatment from weeks 3 to 5 [SuHx(5W) + Nin]. (C) Examinations of systemic

628 systolic arterial pressure (SAP), heart rate (HR), and body weight in Nx(5W), SuHx(5W),

629 and SuHx(5W) + Nin rats. Plotted values are means ± SE (n=5). * p<0.05. ** p<0.001. ***

630 p<0.0005, **** p<0.0001.

631

632 Figure 4. Effect of chronic nintedanib for the remodeling of small pulmonary arteries.

633 (A) Representative elastic Van Gieson staining of pulmonary arteries in pulmonary

634 normotensive control rats [Nx(5W)], Sugen 5416/hypoxic rats at 5 weeks after Sugen 5416

635 injection [SuHx(5W)], and SuHx rats with nintedanib treatment from weeks 3 to 5 [SuHx(5W)

636 + Nin] (200×). Pulmonary arteries were divided in 50 to 200 μm outer diameter (OD) and <

637 50 μm OD for analysis. Scale bars indicate 50 μm (OD 50-200) and 10 μm (OD < 50). (B)

638 Quantitative analysis of medial wall thickness in pulmonary arteries (left; 50 to 200 μm OD)

639   and intimal occlusive lesions in smaller pulmonary arteries (right, < 50 µm OD) in pulmonary

640   normotensive control rats at 5 weeks [Nx(5W)], Sugen 5416/hypoxic rats at 3 weeks

641   [SuHx(3W)] or at 5 weeks [SuHx(5W)] after Sugen 5416 injection, and SuHx rats with

642   nintedanib treatment from weeks 3 to 5 [SuHx(5W) + Nin]. Grade 0 (no lumen occlusion;

643   white), grade 1 (<50% occlusion; gray), grade 2 (>50% occlusion; black). Plotted values are

644   means ± SE (n=5-6). * $p<0.05$. ** $p<0.001$. *** $p<0.0001$ (left). § $P<0.0001$ vs. Nx(5W). *

645    $p<0.05$ vs. SuHx(3W). # $p<0.001$ vs. SuHx(3W). + $p<0.05$ vs. SuHx(5W) (right).

646

647   Figure 5. Expression of FGF and PDGF receptors in medial and neointimal lesions of small

648   pulmonary arteries.

649   (A) Representative immunohistochemistry of phosphorylated fibroblastic growth factor

650   receptor 1 (pFGFR1) (left side) and phosphorylated platelet derived growth factor

651   receptor-β (pPDGFR-β) (right side) in pulmonary arteries (200×). Scale bars indicate 50

652   µm (OD 50-200) and 10 µm (OD < 50). (B) Quantitative analysis of pFGFR1 and

653   pPDGFR-β levels in pulmonary normotensive control rats at 5 weeks [Nx(5W)], Sugen

654   5416/hypoxic rats at 5 weeks [SuHx(5W)] after Sugen 5416 injection, and SuHx rats with

655   nintedanib treatment from weeks 3 to 5 [SuHx(5W)+Nin]. Pulmonary arteries were divided

656   into 50 – 200 µm outer diameter (OD) and < 50 µm OD for analysis. Plotted values are

657   means ± SE (n=5). * p<0.0001 vs. Nx. + p<0.01 vs. Nx. # p<0.05 vs. SuHx(5W).

658

659   Figure 6. Expression of Twist1 protein in lung tissue of rats.

660   Expression of Twist1 protein by western blotting analysis in lung tissues from pulmonary

661   normotensive control rats at 5 weeks (Nx), Sugen 5416/hypoxic rats at 5 weeks [SuHx(5W)]

662   after Sugen 5416 injection, and SuHx rats with nintedanib treatment from weeks 3 to 5

663   [SuHx(5W) + Nin]. Representative blots are shown (left). Protein signals were quantified by

664   densitometric analysis, normalized to the corresponding β-actin signal, and plotted as fold

665   changes (right). The plotted values shown are means ± SE (n=5). * p<0.001 vs. CON. #
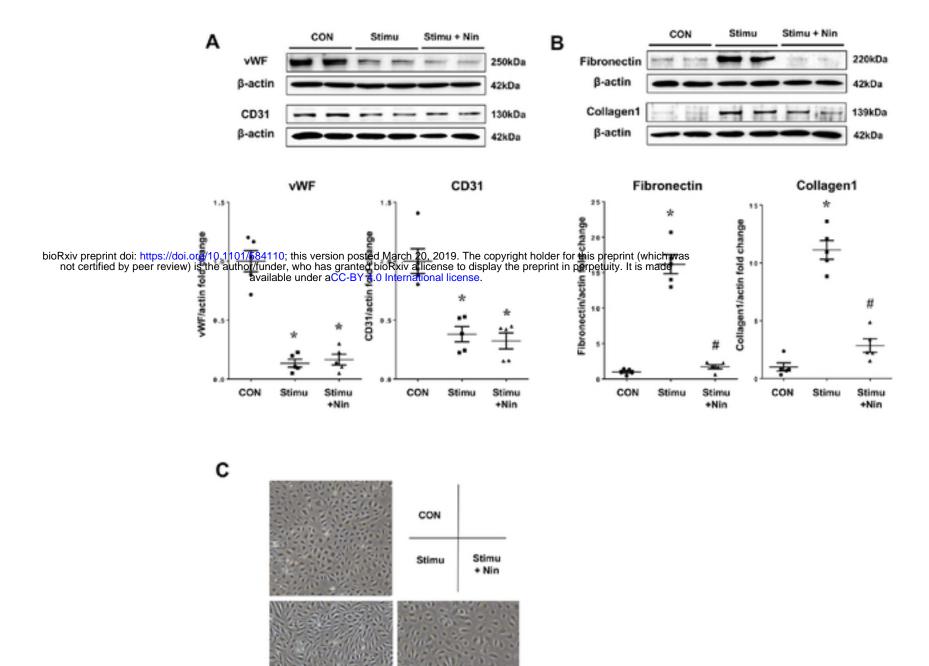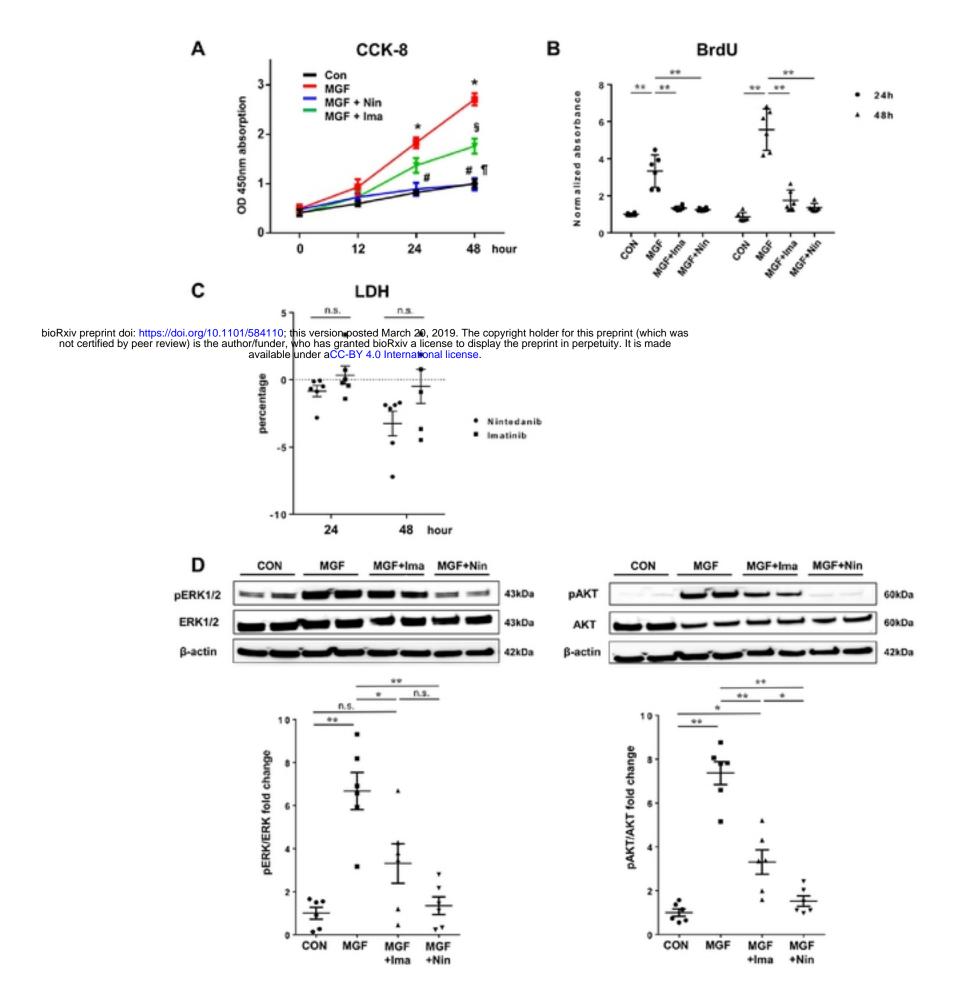
666   p<0.05 vs. SuHx(5W).

Figure 1.

Figure1

Figure 2.

A CCK-8

B BrdU

C LDH

D

Figure2

Figure 3.

Figure3

Figure 4.

A

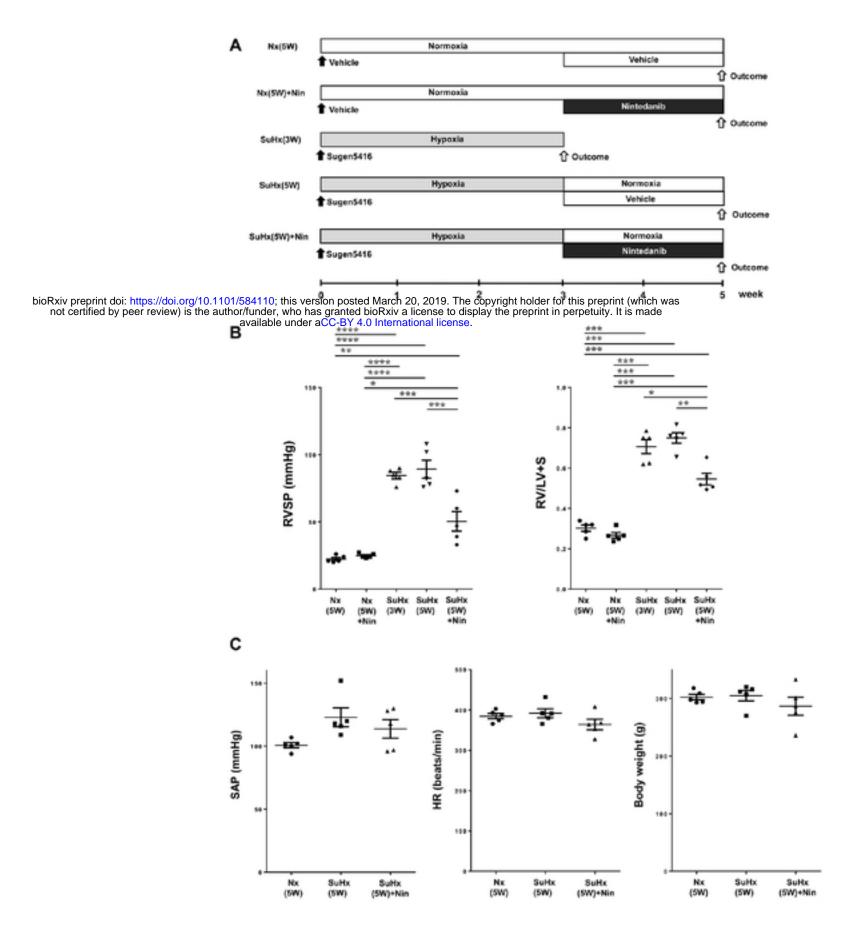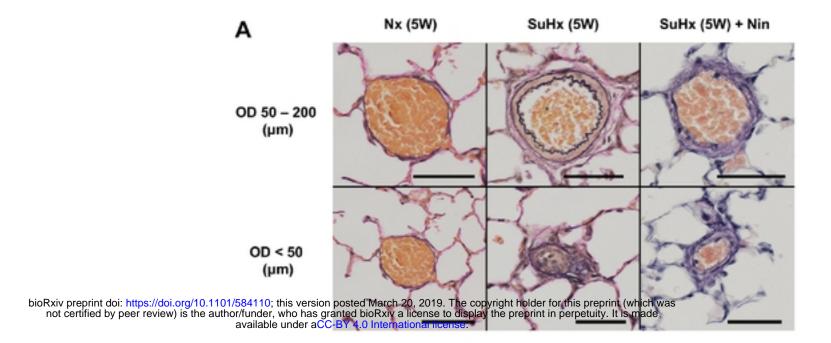|	Nx (5W)	SuHx (5W)	SuHx (5W) + Nin
OD 50 – 200 (μm)			
OD < 50 (μm)			

B

OD 50 – 200 (μm)

OD < 50 (μm)

Figure4

Figure 5.

Figure5

Figure 6.

Figure6